APRIL 07 2016

Normal mode solutions for seismo-acoustic propagation resulting from shear and combined wave point sources

Jennifer L. Nealy; Jon M. Collis; Scott D. Frank

J. Acoust. Soc. Am. 139, EL95–EL99 (2016)
https://doi.org/10.1121/1.4944752

Normal mode solutions for seismo-acoustic propagation resulting from shear and combined wave point sources

Jennifer L. Nealy and Jon M. Collis[a)]
Department of Applied Mathematics and Statistics, Colorado School of Mines, Golden, Colorado 80401, USA
jenniferleighnealy@gmail.com, jon.collis@ll.mit.edu

Scott D. Frank[b)]
Department of Mathematics, Marist College, 3399 North Road, Poughkeepsie, New York 12601, USA
Scott.Frank@marist.edu

Abstract: Normal mode solutions to range-independent seismo-acoustic problems are benchmarked against elastic parabolic equation solutions and then used to benchmark the shear elastic parabolic equation self-starter [Frank, Odom, and Collis, J. Acoust. Soc. Am. **133**, 1358–1367 (2013)]. The Pekeris waveguide with an elastic seafloor is considered for a point source located in the ocean emitting compressional waves, or in the seafloor, emitting both compressional and shear waves. Accurate solutions are obtained when the source is in the seafloor, and when the source is at the interface between the fluid and elastic layers.

[DD]
Date Received: September 1, 2015 **Date Accepted:** March 14, 2016

1. Introduction

Normal mode solutions for the acoustic field in an ocean acoustic environment overlying an elastic halfspace (the *elastic Pekeris waveguide*) have recently been verified using laboratory data.[1] An alternate solution approach using a Green's function was also verified for the case where an acoustic source is located in the water column.[2] Those results did not consider the more complicated case of a point source located in the elastic layer, where it would generate some combination of compressional and shear waves.[3] This work generalizes the previous Green's function approach for the elastic Pekeris waveguide to obtain acoustic field solutions for the cases where a point source is located inside the elastic layer and where a point source is on the boundary between the two media.

Normal mode acoustic field solutions are benchmarked using elastic parabolic equation solutions known to be accurate when a compressional wave point source is located in the elastic medium.[4] The normal mode solutions shown here provide a novel opportunity to benchmark the previously unverified parabolic equation shear wave self-starter.[4] This benchmark provides confidence in elastic parabolic equation results for a broad range of seismic source types. For example, the solutions introduced here can be applied to situations that include pile-driving sources, undersea earthquakes, landslides, or volcanic eruptions, all of which are seismic sources that are not purely compressional in nature. In addition, acoustic field results from a source located precisely at the seafloor interface are obtained by the normal mode solution, something that parabolic equation solutions cannot currently provide. This paper outlines normal mode solutions obtained using Green's functions for compressional and shear components of an elastic source. Examples that demonstrate the accuracy of the solutions, as well as the accuracy of the shear wave elastic parabolic equation self-starter are presented and discussed.

2. Normal mode solution technique

Consider a time-harmonic point source within the elastic Pekeris waveguide with a water column of depth H, constant compressional wave speed c_1, and density ρ_1. An elastic halfspace of constant density ρ_2 with compressional wave speed c_2 and shear

[a)]Present Address: Lincoln Laboratory, Massachusetts Institute of Technology, Lexington, MA 02420, USA.
[b)]Author to whom correspondence should be addressed.

wave speed c_s is below the water column. An azimuthally symmetric cylindrical geometry in a range-independent environment is assumed. Coordinate axes are oriented such that the depth z is positive downward and r is the radial distance from the z axis. For the cases considered, the point source has angular frequency ω, scalar strength S_ω, and lies on the z axis at position $(r, z) = (0, z_s)$.

The acoustic field is represented using a compressional potential in the water column ϕ_1, a compressional potential in the sediment layer ϕ_2, and a shear potential in the sediment layer ψ_2. These potentials are written in terms of the inverse Hankel transform, summed over all possible wavenumbers:

$$\varepsilon(r,z) = \frac{1}{2}\int_{-\infty}^{\infty} \varepsilon'(k_r,z) H_0^{(1)}(k_r r) k_r dk_r, \tag{1}$$

for k_r the horizontal wavenumber, $H_0^{(1)}$ the Hankel function of the first kind, and ε representing one of the potentials. Vertical wavenumbers are defined in terms of the medium and horizontal wavenumbers,

$$k_{z,1} = \sqrt{k_1^2 - k_r^2} \quad \text{and} \quad k_{z,j} = \begin{cases} \sqrt{k_j^2 - k_r^2}, & |k_r| < |k_j|, \\ i\sqrt{k_r^2 - k_j^2}, & |k_r| > |k_j|, \end{cases} \tag{2}$$

for $j = 2, s$. The subscripts (1) and (2) indicate quantities associated with the compressional field in the water or sediment layer, respectively, and the subscript (s) represents a quantity associated with the shear field. The $k_{z,j}$ terms are defined such that the radiation condition of no incoming waves at infinity is satisfied.

The normal and tangential stresses are defined in terms of displacements by

$$\sigma_{zz} = \lambda \nabla^2 \phi + 2\mu \frac{\partial w}{\partial z}, \quad \sigma_{zr} = \mu\left(\frac{\partial u}{\partial z} + \frac{\partial w}{\partial r}\right), \tag{3}$$

for Lamé constants λ and μ.[5,6] The vertical and horizontal displacements, w and u, can be written in terms of the range and depth-dependent displacement potentials as[5,6]

$$\begin{aligned} u_1 &= \frac{\partial \phi_1}{\partial r}, \quad w_1 = \frac{\partial \phi_1}{\partial z}, \\ u_2 &= \frac{\partial \phi_2}{\partial r} + \frac{\partial^2 \psi_2}{\partial r \partial z}, \quad w_2 = \frac{\partial \phi_2}{\partial z} + \frac{\partial^2 \psi_2}{\partial z^2} + k_s^2 \psi_2. \end{aligned} \tag{4}$$

Medium wavespeeds are related to the Lamé parameters by $c_j = \sqrt{\lambda_j + 2\mu_j/\rho_j}$, $j = 1, 2$, and $c_s = \sqrt{\mu_2/\rho_2}$, where the shear modulus μ is zero in the fluid layer. Complex wave speeds, $C_2 = c_2/(1 + i\eta\alpha_p)$ and $C_s = c_s/(1 + i\eta\alpha_s)$ are used to account for absorption losses in the bottom layer where α_p and α_s are the compressional and shear wave attenuations, in decibels per wavelength, and $\eta = (40\pi \log_{10} e)^{-1}$.[7] Compressional and shear waves have corresponding medium wavenumbers $k_1 = \omega/c_1$, $k_2 = \omega/C_2$, and $k_s = \omega/C_s$.

At the water's surface there is a pressure release boundary, meaning that $\phi_1 = 0$ at $z = 0$ m. At the interface between the water and elastic layers, continuity of vertical displacement, continuity of normal stress, and zero tangential stress, are required at $z = H$:

$$(\sigma_{zz})_1 = (\sigma_{zz})_2 \quad \text{and} \quad w_1 = w_2 (\sigma_{zr})_2 = 0. \tag{5}$$

The Green's function solution presented here allows a point source to emit compressional waves when the source is in the water column as well as any combination of compressional and shear waves when the source is in the elastic layer. The point source can be placed at the interface between the water column and the sediment layer. The Green's function is given by

$$G = \frac{S_\omega}{4\pi i k_{z,j}} e^{ik_{z,j}|z - z_s|}, \tag{6}$$

for $j = 1, 2, s$, and is dependent on source depth and the horizontal wavenumber. In order to represent all possible source locations when deriving normal mode solutions, the symbolic forms of the functions associated with each potential are left in the equations for the displacement potentials through the derivation. The Green's function corresponding to

the compressional potential in the water is denoted G_{cw}, and those corresponding to the compressional and shear potentials in the sediment layer as G_{cb} and G_s.

Depth-dependent potentials are given by

$$\begin{aligned}\phi'_1(k_r,z) &= G_{cw}(k_r,z) + Ae^{ik_{z,1}z} + Be^{-ik_{z,1}z},\\ \phi'_2(k_r,z) &= G_{cb}(k_r,z) + Ce^{ik_{z,2}(z-H)},\\ \psi'_2(k_r,z) &= G_s(k_r,z) + De^{ik_{z,s}(z-H)},\end{aligned} \tag{7}$$

for amplitude coefficients A, B, C, and D that are dependent on the horizontal wavenumber.

Applying boundary and interface conditions results in a system of four equations with four unknowns that can be written in matrix-vector form as $M\boldsymbol{x} = \boldsymbol{b}$, where M is a constant coefficient matrix, $\boldsymbol{x}$ is a vector containing amplitude coefficients, and $\boldsymbol{b}$ is a vector containing the Green's functions in Eq. (7) with the boundary conditions applied.

Performing row reduction on the augmented matrix $[M|\boldsymbol{b}]$ determines the amplitude coefficients. In the case of ϕ'_1, plugging the coefficients into the equation for the potential results in

$$\begin{aligned}\phi'_1(k_r,z) = \frac{-1}{if(k_r)}\Bigg\{&-G_{cw}if(k_r) + i\sin(k_{z,1}z)\Bigg[iC_s^2\rho_2\left[\left(2k_r^2-k_s^2\right)^2 + 4k_r^2k_{z,2}k_{z,s}\right]\\ &\times(-G_{cw_2}+G_{cb_2}+G_{s_2}) + k_{z,2}k_s^2\left(-\omega^2\rho_1G_{cw_3} + G_{cb_3} - 2C_s^2\rho_2G_{s_3}\right)\\ &-iC_s^2k_r^2\rho_2\left[2k_r^2 + 2k_{z,2}k_{z,s} - k_s^2\right](G_{s_4}+2G_{cb_4})\Bigg]\\ &+iG_{cw_1}\Bigg[i\cos\left(k_{z,1}[z-H]\right)\left(k_{z,1}\rho_2\left[\left(2k_r^2-k_s^2\right)^2 + 4k_r^2k_{z,2}k_{z,s}\right]\right)\\ &+k_{z,2}k_s^4\rho_1\sin\left(k_{z,1}[z-H]\right)\Bigg]\Bigg\},\end{aligned} \tag{8}$$

where

$$f(k_r) = \rho_1\omega^2k_s^2k_{z,2}\sin(k_{z,1}H) + i\rho_2C_s^2k_{z,1}[4k_r^2k_{z,2}k_{z,s} + (2k_r^2-k_s^2)^2]\cos(k_{z,1}H) \tag{9}$$

is the characteristic equation used to determine horizontal wavenumbers. The roots of this environment specific function are necessary for obtaining representations for the acoustic field potential in the water and compressional and shear potentials in the elastic seafloor. Roots are used to construct normal mode representations for energy propagating in the fluid layer without significant loss. Since Eq. (9) has been written such that it does not have poles, the winding integral root-finding technique developed by McCollom *et al.* is applied to determine horizontal wavenumbers in the complex plane.[2]

Modal sum representations for each of the three potentials are found by applying the residue theorem and using the Ewing-Jardetsky-Press integration contour and branch cuts, resulting in analytic expressions for each potential.[2,5,6] For example, $\phi_1(r,z)$ is found to be

$$\begin{aligned}\phi_1(r,z) = \pi i\sum_{n=1}^{\infty}\frac{H_0^{(1)}\left(k_r^{(n)}r\right)k_r^{(n)}}{f'\left(k_r^{(n)}\right)}\Bigg\{&-\sin\left(k_{z,1}^{(n)}z\right)\Bigg[iC_s^2\rho_2\left[\left(2\left(k_r^{(n)}\right)^2-k_s^2\right)^2 + 4\left(k_r^{(n)}\right)^2k_{z,2}^{(n)}k_{z,s}^{(n)}\right]\\ &\times(-G_{cw_2}+G_{cb_2}+G_{s_2}) + k_{z,2}^{(n)}k_s^2\left(-\omega^2\rho_1G_{cw_3} + G_{cb_3} - 2C_s^2\rho_2G_{s_3}\right)\\ &-iC_s^2\left(k_r^{(n)}\right)^2\rho_2\left[2\left(k_r^{(n)}\right)^2 + 2k_{z,2}^{(n)}k_{z,s}^{(n)} - k_s^2\right](G_{s_4}+2G_{cb_4})\Bigg]\\ &-G_{cw_1}\Bigg[i\cos\left(k_{z,1}^{(n)}[z-H]\right)\left(k_{z,1}^{(n)}\rho_2\left[\left(2\left(k_r^{(n)}\right)^2-k_s^2\right)^2 + 4\left(k_r^{(n)}\right)^2k_{z,2}^{(n)}k_{z,s}^{(n)}\right]\right)\\ &+k_{z,2}^{(n)}k_s^4\rho_1\sin\left(k_{z,1}^{(n)}[z-H]\right)\Bigg]\Bigg\},\end{aligned} \tag{10}$$

where vertical wavenumbers given in terms of the nth horizontal wavenumber $k_r^{(n)}$ are $k_{z,1}^{(n)}$, $k_{z,2}^{(n)}$, and $k_{z,s}^{(n)}$, and $f'(k_r)$ is the first derivative of $f(k_r)$. Similar summation

solutions are found for ϕ_2 and ψ_2, though are not given here. The Green's functions used in Eq. (10) are defined as

$$G_{cw_1} = G_{cw}|_{z=0}, \quad G_{cw_2} = \frac{\partial G_{cw}}{\partial z}\bigg|_{z=H}, \quad G_{cw_3} = G_{cw}|_{z=H},$$
$$G_{cb_2} = \frac{\partial G_{cb}}{\partial z}\bigg|_{z=H}, \quad G_{cb_3} = \left[\lambda_2 k_2^2 - 2\mu_2 \frac{\partial^2}{\partial z^2}\right] G_{cb}|_{z=H}, \quad G_{cb_4} = \frac{\partial G_{cb}}{\partial z}\bigg|_{z=H},$$
$$G_{s_2} = \left[\frac{\partial^2}{\partial z^2} + k_s^2\right] G_s|_{z=H}, \quad G_{s_3} = \left[\frac{\partial^3}{\partial z^3} + \frac{\partial}{\partial z} k_s^2\right] G_s|_{z=H}, \quad G_{s_4} = \left[2\frac{\partial^2}{\partial z^2} + k_s^2\right] G_s|_{z=H}, \quad (11)$$

where vertical lines indicate evaluation at specific depth values. Once the horizontal wavenumber roots have been found, Eq. (10) is used to calculate the acoustic field in the water.

3. Examples

To demonstrate the accuracy of the Green's function approach for shear sources, consider a source emitting compressional and shear waves in the sediment layer. Transmission loss (TL) is used to validate the normal mode solution against an elastic parabolic equation (EPE) solution. The accuracy of EPE solutions have been established previously using wavenumber integration solutions for a purely compressional source. The normal mode solution will be used to provide a previously unavailable benchmark for the accuracy the EPE shear wave self-starter.[4] A second example demonstrates normal mode solutions for a source emitting shear and compressional waves at the fluid-elastic interface.

When the Green's function solution is constructed, a combination of the Green's functions G_{cw}, G_{cb}, and G_s will be used in Eq. (7). Varying the values of these parameters results in solutions for weighted versions of seismic sources. For example, to represent the solution from a 100% compressional source in an elastic layer, G_{cb} is multiplied by a unit weighting term and G_s and G_{cw} are multiplied by zero weighting terms. For the cases considered here, the, normal mode solutions are benchmarked against an EPE solution. Note that the decomposition of seismic sources into shear and compressional components is outlined in Aki and Richards.[3]

Figure 1 compares normal mode solutions (dashed curves) against EPE solutions (solid curves) for the case where a point source in a sediment layer emits different percentages of shear and compressional waves. The environment is a 500 m fluid layer over an elastic halfspace where $c_w = 1500\,\text{m/s}$, $c_2 = 1700\,\text{m/s}$, $c_s = 800\,\text{m/s}$, and density $\rho = 2\,\text{g/cm}^3$. Attenuation in the halfspace is $\alpha_p = 0.1$ and $\alpha_s = 0.2$ dB/wavelength. The solutions are compared at a frequency of 15 Hz with a source depth of $z_s = 600\,\text{m}$ and a receiver depth of $z_r = 200\,\text{m}$. Figure 1(a) compares the normal mode solution for a 100% compressional source to an EPE solution using the 100% compressional self-starter. Since the self-starter has been previously benchmarked, this confirms the accuracy of the Green's function solution. Figure 1(b) compares the normal mode and EPE solutions with 100% shear wave sources and serves as a previously unobtainable benchmark of the shear wave self-starter.[4] Figure 1(c) demonstrates a combined source using 50% compressional and 50% shear wave source terms. In all three comparisons,

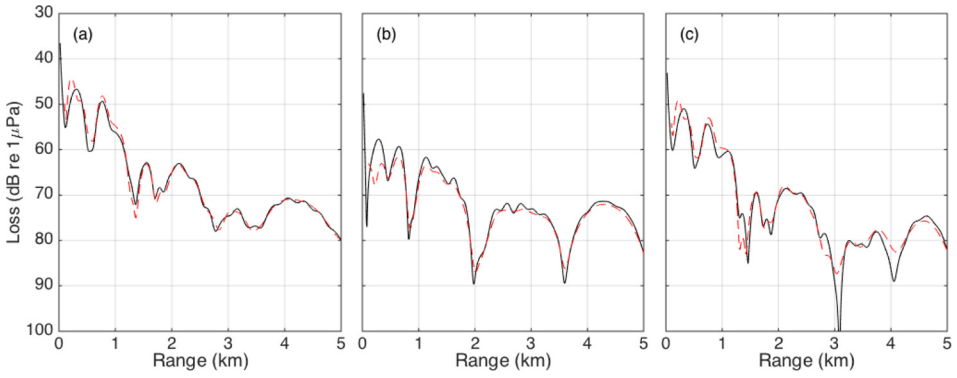

Fig. 1. (Color online) Transmission loss versus range for a 500 m depth range-independent waveguide with source frequency 15 Hz, source depth of $z_s = 600\,\text{m}$ and a receiver depth of $z_r = 200\,\text{m}$. The solid lines represent solutions from the elastic parabolic equation and the dashed lines show the Green's function solution from Eq. (7) for a point source in the sediment emitting (a) 100% compressional waves, (b) 100% shear waves, and (c) 50% compressional and 50% shear waves.

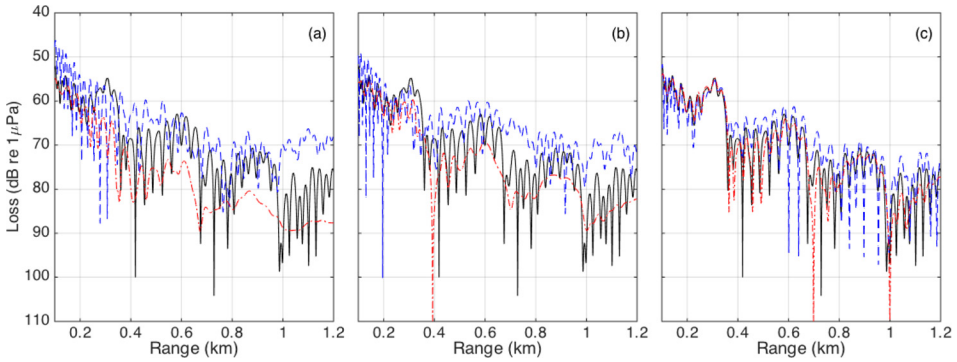

Fig. 2. (Color online) Transmission loss versus range for a range-independent environment with source frequency of 180 Hz and a receiver depth of $z_r = 137.1$ m. The solid lines show the normal mode solution for a point source at the interface, dashed lines show solutions for a source above the interface, and dash-dotted lines correspond to solutions for a source below the interface. Distances of each source from the interface are (a) 10 m, (b), 5 m, and (c) 1 m.

there is excellent agreement in both pattern phase and amplitude. Note the EPE solution includes all evanescent modes near the source, which accounts for small variations at short range.

Figure 2 compares normal mode solutions for a source at the fluid-elastic interface (solid curve) to those for sources just above (dashed curve) and just below (dashed-dotted curve) the interface. The environment is range independent, with a 150 m thick water column with a 1482 m/s isospeed profile. The elastic halfspace has $c_2 = 2290$ m/s, $c_s = 1050$ m/s, $\rho = 1.378$ g/cm^3. Attenuation parameters are $\alpha_p = 0.76$ and $\alpha_s = 1.05$ dB/wavelength. In this example the sources are emitting purely compressional waves in both the water column and the sediment layer. In Fig. 2, the distance of the sources above or below the seafloor are (a) 10 m, (b) 5 m, and (c) 1 m. The receiver depth of $z_r = 137.1$ m is chosen to be consistent with results from previous studies of normal mode solutions.[2] The consistency of the transition serves to confirm the interface source model.

4. Discussion

The solution presented herein allows for a combination of seismic source terms to be used in varying proportions and allows for solutions where there is a point source emitting both compressional and shear waves. The accuracy of the normal mode solution for point sources with shear and combined waves in elastic sediments was demonstrated. This solution is capable of modeling a point source at the seafloor interface, producing shear waves in the sediment layer and compressional waves in both the water column and the seafloor. This technique can be extended for use to other ocean acoustic problems such as the elastic Pekeris waveguide with an overlying ice layer.

Acknowledgments

This work was supported by an Office of Naval Research grant to Marist College and by a grant from the Simons Foundation (Grant No. 279472 to S.D.F.).

References and links

[1]J. D. Schneiderwind, J. M. Collis, and H. J. Simpson, "Elastic Pekeris waveguide normal mode solution comparisons against laboratory data," J. Acoust. Soc. Am. **132**, EL182–EL188 (2012).
[2]B. A. McCollom and J. M. Collis, "Root finding in the complex plane for seismo-acoustic propagation scenarios with Green's function solutions," J. Acoust. Soc. Am. **136**, 1036–1045 (2014).
[3]K. Aki and P. G. Richards, *Quantitative Seismology* (University Science Books, South Orange, NJ, 2002), Vol. 1, Chaps. 3, 4.
[4]S. D. Frank, R. I. Odom, and J. M. Collis, "Elastic parabolic equation solutions for underwater acoustic problems using seismic sources," J. Acoust. Soc. Am. **133**, 1358–1367 (2013).
[5]F. B. Jensen, W. A. Kuperman, M. B. Porter, and H. Schmidt, *Computational Ocean Acoustics*, 2nd ed. (Springer Science+Business Media, New York, 2011), Chaps. 2, 5.
[6]M. Ewing, W. Jardetsky, and F. Press, *Elastic Waves in Layered Media*, 1st ed. (McGraw-Hill, New York, 1957), Chaps. 1, 2.
[7]M. D. Collins, "A higher-order parabolic equation for wave propagation in an ocean overlaying an elastic bottom," J. Acoust. Soc. Am. **86**, 1459–1464 (1989).